AN IMPROVED INTERACTIVE BUCKLING ANALYSIS OF THIN-WALLED COLUMNS HAVING DOUBLY SYMMETRIC SECTIONS

SRINIVASAN SRIDHARAN† and M. ASHRAF ALI‡

Department of Civil Engineering, Washington University, St. Louis, MO 63130, U.S.A.

Abstract—A comprehensive mode interaction analysis is presented for thin-walled columns having doubly symmetric cross-sections and carrying axial compression. It is shown that as a result of interaction of overall bending with the primary local mode, a "secondary" local mode having the same wavelength as the primary, is triggered. The problem is therefore viewed as one of interaction of three modes: viz. the overall (Euler) buckling mode and the two local modes. The analysis is based on Koiter's theory of mode interaction and employs finite strips to describe local buckling deformation. The column is treated as being loaded by a prescribed end compression at the centroid and a suitably prescribed end rotation to maintain concentricity of load application. Examples are presented to compare the results of the present theory with the currently available analytical results and to examine the behavior of typical cross-sections. Of particular interest is the considerably reduced imperfection-sensitivity of columns with well-separated critical stresses in comparison to that reported earlier in published literature.

NOTATION

The most important symbols are listed below:

A	area of cross-section	t_w	thickness of web of I-section
B	width of flange of I-section, width of panel in stiffened plate	t_s	thickness of stiffener for the stiffened plate
D	depth of web of I-section, depth of stiffener in stiffened plate, also flexural rigidity of a plate $[= Et^3/12(1-v^2)]$	u, v, w	the middle surface displacements in the axial, transverse and normal directions referred to a plate element
E	Young's modulus	x, y	axial and transverse coordinates for a plate element
N_x, N_y, N_{xy}	inplane stress resultants (normal force in the axial and transverse directions and shear force)	Π	potential energy function
		$\varepsilon_x, \varepsilon_y, \varepsilon_{xy}$	tensor strain components
I	the second moment of the area of the cross-section about the weaker axis	λ	end compression (total axial shortening/l)
W	overall deflection of the cross-section perpendicular to the weaker axis	v	Poisson's ratio
Z	distance of a point on the plate middle surface from the weaker axis	$\zeta_1, \zeta_2, \zeta_3$	the scaling factors for the overall, the primary local and the secondary local modes, respectively (maximum deflection divided by t)
l	length of the plate structure	$\bar{\zeta}_1, \bar{\zeta}_2, \bar{\zeta}_3$	dimensionless initial imperfection amplitudes (maximum initial imperfection amplitude divided by t)
m	number of half waves of local buckling		
r	radius of gyration of the square box section	$\bar{\zeta}_1^*$	$\bar{\zeta}_1 \times l/(l/1000)$
t	thickness of a typical plate element (thickness of flange in the I-section, thickness of main plate in stiffened panel)	$\sigma_{c_1}, \sigma_{c_2}, \sigma_{c_3}$	magnitudes of critical stresses in the three modes
		σ_u	the maximum average stress that a column section can carry

INTRODUCTION

It is well known that nonlinear mode interaction of local and overall (Euler type) buckling modes is the principal cause of collapse of thin-walled columns. The phenomenon is imperfection sensitive particularly when the critical stresses for the two modes are near coincident.

† Associate Professor.
‡ Doctoral Candidate.

Though a wealth of literature is available on the subject, there persists some controversy over the quantitative estimates of imperfection sensitivity and the maximum load a given thin-walled column can support. van der Neut's analytical model[1], the discussion of erosion of the "naive" optimum by Thompson and Lewis[2], Graves-Smith's investigation of box columns[3] and Tvergaard's analysis of stiffened panels[4] constitute some of the major landmarks in this field. A thorough analysis of stiffened panels[5, 6] was performed by Koiter and Pignataro. The method is asymptotic but is well suited for relatively large imperfections. However, the analysis is not applicable for doubly symmetric cross-sections as then the coefficient of the $\xi_1\xi_2^2$ term in the energy expression (ξ_1 and ξ_2 being the scaling factors of the overall and local modes, respectively)—the key term governing the inter-action—vanishes. In order to deal with this situation, Koiter and van der Neut[7] proposed a technique in which the interaction of an overall mode with two local modes was considered. A number of examples of practical interest were studied.

A major difficulty in the asymptotic analysis of a column with two axes of symmetry for an interaction of the fundamental local mode (henceforth called "primary") and the overall mode arises in the following manner: the coefficients of the cubic terms in the energy expression, viz. ξ_1^3 and $\xi_1\xi_2^2$ vanish; the interaction then hinges on the $\xi_1^2\xi_2^2$ term which cannot be correctly evaluated without the consideration of the mixed second order field; the latter takes on essentially the character of a local mode (henceforth called "secondary") having the same wavelength as the primary local mode (this is demonstrated in the present paper). The eigenvalue of the secondary local mode can be sufficiently close to that of the primary mode to give rise to a singularity in the evaluation of the mixed second order field[8, 9], thus throwing a doubt on the final results.

The solution to this problem is, however, simple: treat the (secondary) local mode which makes its appearance as the mixed second order field as one of the principal modes participating in the interaction. Thus there would be three degrees of freedom in the problem, viz. ξ_1, ξ_2 and ξ_3, the last one being the scaling factor corresponding to the secondary local mode. The mixed second order field associated with bilinear term $\xi_1\xi_2$ would now have to vanish or get essentially "squeezed out" because of the orthogonality condition between each of the second order fields and the eigenmodes[10]. Though not explicitly stated, this indeed is the reasoning behind the 3 mode model proposed by Koiter and van der Neut[7].

The problem posed by the said singularity was bypassed in the earlier work of Sridharan[8] and Sridharan and Benito[9] by simply neglecting a key term associated with the load parameter (λ) in the evaluation of the mixed second order field. The resulting solution was termed an "upper bound" which involved an unquantified error. In the present paper a comprehensive analysis of 3-mode interaction is presented. Some significant features of the approach are described below. In contrast to Ref. [7], where a mechanical model is described, the present authors prefer to deal directly with the plate structure itself. The relevant displacement fields are extracted with ease using a finite strip technique. Since the "exact" displacement functions are used for the description of the longitudinal variation of the displacements, discretization is confined to the transverse direction—where it is most needed—to be able to model complex cross-sectional configurations. In particular, the mixed second order field (associated with the $\xi_2\xi_3$ term) neglected in previous work[7] is duly taken into account.

The columns are considered to be simply supported at the ends; the column cross-sections have two axes of symmetry; and the column is loaded by a compressive force passing through the centroid of the end sections. Loading is, however, controlled by the prescription of an end shortening or the average apparent strain (λ) of the column. It is seen that the mixed second order stress field (associated with $\xi_2\xi_3$) in the form which satisfies differential equations of equilibrium, introduces moments at the end sections and thus the resultant force no longer passes through the centroid. A secondary loading parameter is therefore introduced which is a suitably prescribed end rotation to ensure the concentric application of the end compression. Note this technique has been used in the post-local-buckling analysis of plate structures subject to compressive loads having pre-scribed eccentricity[11, 12].

In the following sections, the theoretical basis of the present approach is briefly discussed and some typical examples are considered.

THEORY

General

The method of approach consists of the following steps:

(i) Solving for the following field problems:

(a) the eigenvalue problems for the participating modes of buckling, viz. the two companion local modes and the overall mode; and

(b) the respective second order displacement fields in the individual modes as well as the mixed second order field arising out of the interaction of the two local modes.

The sufficiency of the second order fields in (b) for a full description of the interaction is discussed in a later section.

(ii) Developing a potential energy function in terms of (ξ_1, ξ_2, ξ_3) the scaling factors of the modes, $(\bar{\xi}_1, \bar{\xi}_2, \bar{\xi}_3)$ the scaling factors associated with initial imperfections assumed to take the form of modes of buckling and (λ, χ) the load parameters corresponding to axial compression and end rotation.

(iii) The solution of the nonlinear equations using a standard numerical technique such as the Newton–Raphson procedure.

Local buckling deformation in individual modes

The local buckling deformations are modelled using the "classical assumptions" introduced by Benthem[13]. These are (Fig. 1):

(i) At a corner or a plate junction where two plates meet at an angle, the normal displacement for each plate vanishes.

A consequence of this assumption is that the local buckling problem becomes inextensional to the first order so that the buckling mode for the column can be described taking for each strip

$$w_i = \bar{w}_i(y) \sin\left(\frac{m\pi x}{l}\right),$$ (1a)

$$i = 2, 3,$$

$$u_i = v_i = 0,$$ (1b)

where m is the number of half waves of buckling (the same for the two local modes as
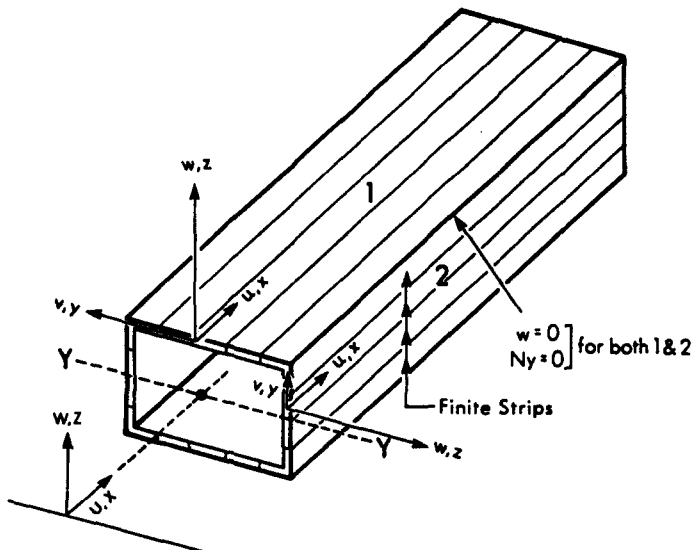

Fig. 1. Local and global coordinate systems and finite strip configuration.

discussed later), l is the length of the plate structure, i identifies a certain local mode, and $\bar{w}(y)$ is an appropriate function of y, the transverse coordinate.

(ii) The normal stress resultant in the transverse direction, N_y, vanishes for each plate meeting at the corner.

This assumption together with (i) eliminates coupling of the inplane and out of plane displacements and stress resultants in the plate structure, so that the second order displacement field can be represented in the form:

$$u_{ii} = \bar{u}_{ii}(y) \sin\left(\frac{2m\pi x}{l}\right), \tag{2a}$$

$$v_{ii} = \bar{v}_{ii,0}(y) + \bar{v}_{ii,2}(y) \cos\left(\frac{2m\pi x}{l}\right) \quad \text{(no sum on } i\text{)}, \tag{2b}$$

$$w_{ii} = 0, \qquad\qquad i = 2, 3. \tag{2c}$$

Thus in a single mode local buckling problem

$$u = u_0 + u_{ii}\xi_i^2,$$

$$v = v_0 + v_{ii}\xi_i^2 \quad \text{(no sum on } i\text{)},$$

$$w = w_i\xi_i, \tag{3a–c}$$

where ξ_i is the scaling factor and (u_0, v_0) are the prebuckling displacements given by $\partial u_0/\partial x = -\lambda$, $\partial v_0/\partial y = \nu\lambda$. The eigenmodes and the respective second order fields are determined with ease invoking the appropriate potential energy functions[8] and using the finite-strip method developed in Ref. [14].

Overall buckling deformation

Euler type overall buckling is modelled simply by using the Euler–Bernoulli hypothesis, so that the lateral deflection of the entire cross-section is given by that of the centroidal line. Thus the buckling mode is represented by

$$W_1 = \bar{W}_1 \sin\left(\frac{\pi x}{l}\right). \tag{4}$$

The subscript 1 is used to signify the quantities associated with overall buckling. $\bar{W}_1$ is the central deflection measured perpendicular to the weaker axis of the column section.

The second order field consists essentially of axial displacement ($U_{11} \equiv u_{11}$) which is constant across the section and given by

$$U_{11} = -\frac{\pi}{8l}\bar{W}_1^2 \sin\left(\frac{2\pi x}{l}\right). \tag{5}$$

Thus under the action of overall buckling alone, the column axis remains unstrained and the end shortening due to buckling (Δ_{11}) is given by

$$\lambda_{11} = \frac{\Delta_{11}}{l} = \frac{\pi^2}{4}\left(\frac{\bar{W}_1^2}{l^2}\right). \tag{6}$$

The strains and stresses in the transverse direction are both neglected as in the standard beam theory.

The appearance of a secondary local mode

As the column bends due to overall buckling, the local buckling deformation associated with the primary mode would be considerably modified. Specifically, the displacements on

the compression side of the weaker axis are accentuated while those in the tension side get significantly reduced. The changes of local buckling pattern are attributable to a mixed second order $(\zeta_1\zeta_2)$ field. As mentioned earlier, this takes the character of a local mode (termed "secondary") which has the same wavelength as the primary mode. This is demonstrated in the sequel.

In terms of scaling factors ζ_1 and ζ_2 the middle surface strain components in a 2 mode interaction problem can be written in the form:

$$\begin{Bmatrix} \varepsilon_x \\ \varepsilon_y \\ \gamma_{xy} \end{Bmatrix} = \begin{Bmatrix} \varepsilon_{x_0} \\ \varepsilon_{y_0} \\ 0 \end{Bmatrix} + \begin{Bmatrix} \varepsilon_{x_1} \\ \varepsilon_{y_1} \\ \varepsilon_{xy_1} \end{Bmatrix}\zeta_1 + \begin{Bmatrix} \varepsilon_{x_2} \\ \varepsilon_{y_2} \\ \varepsilon_{xy_2} \end{Bmatrix}\zeta_2 + \begin{Bmatrix} \varepsilon_{x_{11}} \\ \varepsilon_{y_{11}} \\ \varepsilon_{xy_{11}} \end{Bmatrix}\zeta_1^2 + \begin{Bmatrix} \varepsilon_{x_{12}} \\ \varepsilon_{y_{12}} \\ \varepsilon_{xy_{12}} \end{Bmatrix}\zeta_1\zeta_2 + \begin{Bmatrix} \varepsilon_{x_{22}} \\ \varepsilon_{y_{22}} \\ \varepsilon_{xy_{22}} \end{Bmatrix}\zeta_2^2. \qquad (7)$$

The terms ε_{x_0} and ε_{y_0} are the prebuckling strains under uniform compression given by $-\lambda$ and $v\lambda$, respectively. Note also:

$$(i) \qquad \varepsilon_{x_2} = \varepsilon_{y_2} = \varepsilon_{xy_2} = 0, \qquad (8)$$

which follows from eqn (1b)

$$(ii) \qquad \varepsilon_{y_1} = \varepsilon_{xy_1} = 0; \qquad \varepsilon_{x_1} = -ZW_{1,xx}. \qquad (9a,b)$$

These follow from Euler–Bernoulli assumptions governing overall buckling. Z is the distance of any point from the weaker axis

$$(iii) \qquad \varepsilon_{x_{12}} = u_{12,x}; \qquad \varepsilon_{y_{12}} = v_{12,y}; \qquad \varepsilon_{xy_{12}} = \tfrac{1}{2}(u_{12,y} + v_{12,x}). \qquad (10a\text{--}c)$$

(u_{12}, v_{12}, w_{12}) are the displacement components of the mixed second order $(\zeta_1\zeta_2)$ field. In the expression for axial strain term $\varepsilon_{x_{12}}$, a bilinear term of minor significance involving w_2, the normal displacement of plate elements and W_1 (viz. $(\partial W_1/\partial x) \cdot (\partial w_2/\partial x)$) has been neglected for simplicity.

The ordered contributions to the stress-resultants, viz. N_x, N_y and N_{xy}, can now be obtained from the strains using Hooke's law.

The governing differential equations of the mixed second order field can now be obtained by substituting the foregoing expressions in the nonlinear differential equations of the plate structure and equating the coefficients of $\zeta_1\zeta_2$ on both sides of the equation. For the purpose of our demonstration, it is sufficient to take the governing equations as the von Karman plate equations. The following equations result from this operation:

$$u_{12,xx} + \tfrac{1}{2}(1-v)u_{12,yy} + \tfrac{1}{2}(1+v)v_{12,xy} = 0, \qquad (11a)$$

$$v_{12,yy} + \tfrac{1}{2}(1-v)v_{12,xx} + \tfrac{1}{2}(1+v)u_{12,xy} = 0, \qquad (11b)$$

$$D\nabla^4 w_{12} - N_{x_0}w_{12,xx} = N_{x_1}w_{2,xx}. \qquad (11c)$$

In these equations there occurs a decoupling of w_{12} on the one hand, and u_{12}, v_{12} on the other. Equations (11a) and (11b) admit of a solution $u_{12} = v_{12} = 0$. Equation (11c) may be written as

$$D\nabla^4 w_{12} + (\sigma_0 t)w_{12,xx} = -Et\left(\frac{m^2\pi^2}{l^2}\right)W_{1,xx}[Z\bar{w}_2(y)]\sin\left(\frac{m\pi x}{l}\right) \qquad (12)$$

in which $\sigma_0 = E\lambda$, the compressive stress induced in the unbuckled structure, Z is the distance measured perpendicular to the weaker axis. The term enclosed in square brackets
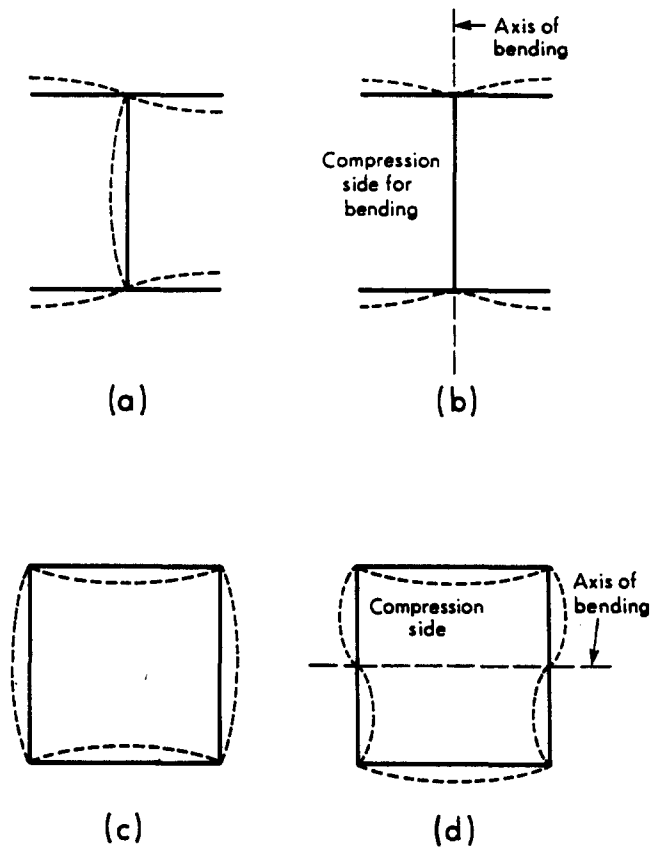
Fig. 2. Typical doubly symmetric sections and the primary and secondary local modes.

is of particular interest here. $\bar{w}_2(y)$ is the variation of local buckling deformation across the section and has a symmetric (or antisymmetric) form with respect to the weaker axis. The product $Z\bar{w}_2(y)$ has therefore an antisymmetric (symmetric) variation with respect to the weaker axis. Now eqn (12) represents a differential equation of an element of a plate structure carrying a certain lateral load which varies nearly sinusoidally in the longitudinal direction and whose variation in the transverse direction takes on an antisymmetric (symmetric) form with respect to the weaker axis of the structure. It is apparent that this load triggers a "secondary" local mode (w_3) whose wavelength is the same as the primary local mode but which takes an antisymmetric (symmetric) form with respect to the weaker axis and this is consistent with the solution $u_{12} = v_{12} = 0$. Figures 2(a)–(d) show typical primary local modes and the corresponding secondary local modes triggered by bending about the weaker axis. As $\sigma_0 \to \sigma_{c_3}$ (σ_{c_3} being the critical stress corresponding to the secondary local mode), w_{12} grows without limit. It is therefore necessary to treat the secondary local mode [which appears as w_{12} in eqn (11c)] as an additional mode participating in the interaction. By an exactly similar reasoning, it can be shown that the character of the mixed second field arising out of the interaction of the overall mode with the secondary local mode is essentially the same as that of the primary local mode.

In order to investigate whether w_{12} is essentially the same as w_3, the w_{12} obtained for the case of a square box column is decomposed into modes of buckling antisymmetric with respect to the weaker axis. Neglecting the effect of the modulating function $W_{1,xx}$ in eqn (12) both w_{12} and the component modes of buckling are deemed to have the same half-wavelength l/m. The first few nontrivial higher modes are shown in Figs. 3(a)–(d). The corresponding critical stresses and the scaling factors in the make up of w_{12} are shown in Table 1.
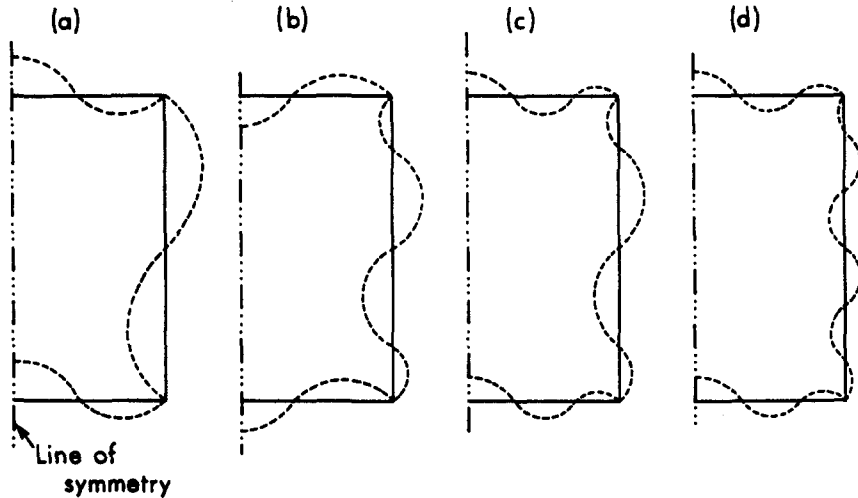
Fig. 3. The higher local modes antisymmetric about the axis of bending.

It is seen from Table 1 that the critical stresses of the higher modes (Fig. 3) are considerably higher than σ_{c_2} or σ_{c_3} and their contribution to w_{12} is also extremely small. It is apparent that under magnitudes of axial compression in the neighborhood of σ_{c_3} these modes will not be triggered and hence may be ignored in calculations of engineering accuracy. Similar conclusions hold good for I-section and other common structural shapes as well. However, a decomposition of w_{12} such as performed here may be necessary for complex structural shapes to assess the possible influence of the higher modes.

Mixed second order fields

In the present analysis therefore the two fundamental local modes (having scaling factors ζ_2 and ζ_3) and their respective second order fields are duly considered. To this, we must add a third one, namely the mixed second order field arising out of the interaction of the two local modes. Since the two local modes are of the same wavelength, it can be shown that the displacement functions which describe this field must be given by expressions of the same form as eqns (2a)–(2c). This field is determined in the same manner as the ζ_2^2 and ζ_3^2 fields.

With the two companion local modes duly accounted for, it is neither necessary nor logical to consider the mixed second order fields arising from an interaction of the overall mode with either of the local modes. This is because each of the second order fields must be orthogonal in some sense to each of the first order fields[10]. As mentioned earlier, the mixed second order displacement fields w_{12} and w_{13} take forms which are little different from the secondary (w_3) and primary (w_2) local modes, respectively; it therefore follows that the former two must be taken to be zero. In other words, the roles of these mixed second order fields are now taken over by the eigenmodes themselves.

Table 1. Data on secondary and higher local modes

Mode designation	Shape (Fig. no.)	Critical stress divided by σ_{c_3}	Relative scaling factors in w_{12}
Secondary (w_3)	Fig. 2(d)	1.43	1.0
Higher modes			
(a)	Fig. 3(a)	8.84	0.021
(b)	Fig. 3(b)	32.96	0.043
(c)	Fig. 3(c)	90.32	−0.008
(d)	Fig. 3(d)	203.50	−0.031

Secondary load parameter

The second order fields cannot depict bending about the weaker axis in the overall sense as each of these must be orthogonal to ξ_1 field. However, in reality there must occur some bending additional to that given by overall buckling in the form of eqn (4). Note that the $\xi_2\xi_3$ stress field produces an axial stress distribution which is antisymmetric with respect to the weaker axis and therefore produces a moment resultant thus shifting the point of application of the axial force from the centroid. Bending of the column in the overall mode given by eqn (4) produces zero axial stresses at the ends of the column and therefore cannot restore the concentricity of load application. This can be achieved only by the introduction of an additional load parameter.

Let the column in its prebuckling state be subjected to a uniform curvature χ in addition to uniform end compression λ. The prebuckling strain field is given by

$$\varepsilon_{x_0} = -\lambda - Z\chi; \qquad \varepsilon_{y_0} = -\nu\varepsilon_{x_0}; \qquad \varepsilon_{xy_0} = 0. \tag{13a–c}$$

Thus χ is an additional load parameter whose function in the present analysis is mainly corrective: at any point on the equilibrium path, χ is *prescribed* suitably so that the resultant of the stresses at the ends of the column passes through the centroid. Thus for a perfect structure

$$\chi = \left\{ \frac{1}{EI} \int_A \sigma_{23} \Big|_{x=0,l} \cdot Z \, dA \right\} \xi_2\xi_3 = \bar{\chi}\xi_2\xi_3, \tag{14}$$

where I is the second moment of the area of the section about the weaker axis and A is the cross-sectional area.

Any destabilizing influence of χ is only in the nature of accentuating the modal amplitudes [cf. terms in square brackets of the potential energy function in eqn (15)]. In this sense χ is not a primary source of instability and hence is termed a secondary load parameter.

Potential energy function

An expression for the total potential energy of the structure can now be written in terms of the scaling factors of the buckling modes, viz. ξ_1, ξ_2, ξ_3, and the two loading parameters (λ and χ). Since the problem is posed as one of prescribed end shortening and end rotation, the potential energy reduces to the internal strain energy. Expressions for the middle surface strain components and the steps leading to the potential energy function are given in the appendix. The function takes the form

$$\Pi = \sum_{i=1,2,3} \left[a_i\left(1 - \frac{\lambda}{\lambda_i}\right)\xi_i^2 - 2a_i \frac{\lambda}{\lambda_i} \xi_i\bar{\xi}_i + b_{ii}\xi_i^2\{\xi_i^2 + 4\xi_i\bar{\xi}_i + 4\bar{\xi}_i^2\} \right]$$

$$+ c\xi_1(\xi_2\xi_3 + \bar{\xi}_2\xi_3 + \xi_2\bar{\xi}_3) + b_{12}(\xi_1^2 + 2\xi_1\bar{\xi}_1)(\xi_2^2 + 2\xi_2\bar{\xi}_2)$$

$$+ b_{13}(\xi_1^2 + 2\xi_1\bar{\xi}_1)(\xi_3^2 + 2\xi_3\bar{\xi}_3) + b_{23}(\xi_2^2 + 2\xi_2\bar{\xi}_2)(\xi_3^2 + \xi_3\bar{\xi}_3)$$

$$+ \lambda\{e_1\xi_1 + e_2(\xi_2\xi_3 + \bar{\xi}_2\xi_3 + \bar{\xi}_3\xi_2)\}, \tag{15}$$

where a_i, b_{ij}, c, e_i are constants; λ_1, λ_2 and λ_3 are the critical values of λ for the three modes of buckling, respectively; and $\bar{\xi}_2 = \bar{\xi}_2$, $\bar{\xi}_3 = \bar{\xi}_3$, but

$$\xi_1 = \dot{\xi}_1 - \underline{\frac{4}{\pi^3} \frac{\chi l^2}{t}} \tag{16}$$

wherein, the underlined term represents the first harmonic contribution of χ to the initial imperfection in the overall mode. (Note that this has been rendered dimensionless by division by t, a characteristic thickness used to render the overall initial imperfection

dimensionless.) The point of major interest here is the presence of the nonvanishing trilinear term $c\xi_1\xi_2\xi_3$ which gives the destabilizing influence of the interaction while b_{12}, b_{13} and b_{23} are the stabilizing terms. In contrast no cubic term could arise in the two-mode analysis (Ref. [9]) of doubly symmetric sections, and its role was performed by a biquadratic term, viz. b_{12} of Ref. [9] and the influences of b_{13} and b_{23} were simply absent.

Tracing the equilibrium path

The equations of equilibrium are produced by setting

$$\frac{\partial \pi}{\partial \xi_i} = 0 \qquad (i = 1, 2, 3) \tag{17}$$

and solved by the Newton–Raphson iterative procedure. At the end of each iteration, χ is computed from

$$\chi = \bar{\chi}(\xi_2\xi_3 + \xi_2\bar{\xi}_3 + \bar{\xi}_2\xi_3) \tag{18}$$

to account for initial imperfections [cf. eqn (14)]. Equilibrium paths were traced incrementing any one of ξ_1, ξ_2, ξ_3 and λ and computing the other three. Stability and bifurcations were inferred from the second variation matrix $[\partial^2\pi/\partial\xi_i\,\partial\xi_j]$ at any point along the equilibrium path.

EXAMPLES

Sample problems are considered in this section to contrast the currently available results with those produced by the present theory and draw some general conclusions on the performance of columns with typical doubly symmetric cross-sections, viz. *I*-section and square box columns and box type stiffened plate panels.

I-Section columns; comparison with Ref. [9]

Figure 4(a) shows the cross-sectional dimensions of *I*-section columns studied. The buckling modes are illustrated in Fig. 2. Twenty-four strips were employed over half the column with advantage taken of the symmetry about the stronger axis. The critical stresses of the two sections considered, viz. (a) and (b), respectively, are given in Table 2. The half-wavelength of local buckling is one corresponding to the lowest value of σ_{c_2}. The length is chosen as a multiple of this half-wavelength.

Imperfection sensitivity at near-coincident buckling is illustrated in Fig. 4(b) for the *I*-section column (a) (case (i) of Table 2). This figure gives the variations of the nondimensional maximum load (σ_u/σ_{c_1}) with overall imperfections for two specific levels of local imperfections, viz. 0 and $0.2t$. These results are compared with those of Ref. [9]. The latter theory neglects the destabilizing influence of the secondary local mode in the evaluation of the mixed second order $(\xi_1\xi_2)$ field. Being a 2-mode formulation, the higher order terms arising out of interaction of the $(\xi_1\xi_2)$ field with the two fundamental modes, which are stabilizing in character, are also neglected. For the near-coincident buckling and for sufficiently small

Table 2. Details of *I*-section columns (Fig. 4(a))

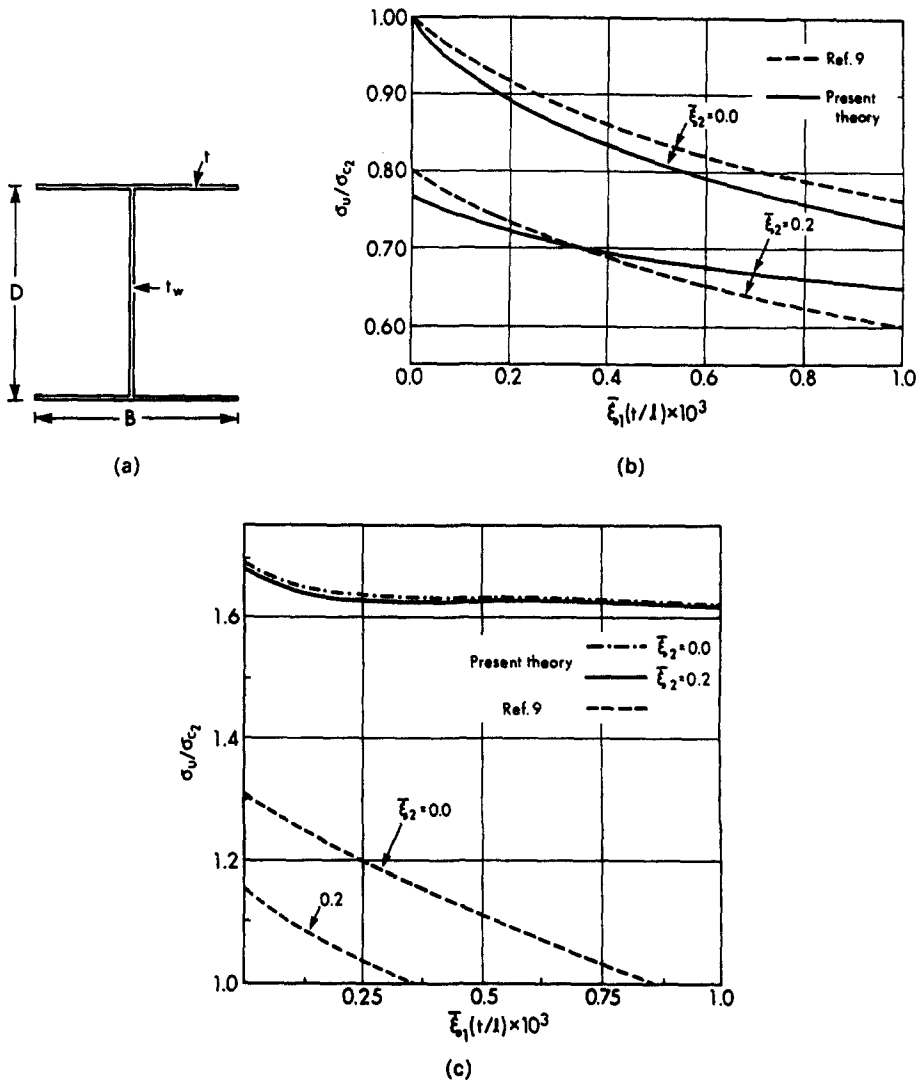| Case	Section	B/t	D/t	t_w/t	l/t	m	$\dfrac{\sigma_{c_1}}{E} \times 10^3$	$\dfrac{\sigma_{c_2}}{E} \times 10^3$	$\dfrac{\sigma_{c_3}}{E} \times 10^3$
(i)	(a)	80	80	2	2000	25	0.656	0.621	0.754
(ii)					1200	15	1.802		
(i)	(b)	80	80	1	3000	25	0.390	0.371	1.042
(ii)					1800	15	1.075		

Fig. 4. (a) Key dimensions of I-section; (b) and (c) dimensionless maximum load vs overall imperfection magnitudes.

imperfections the 2-mode approach of Ref. [9] gives results which are quite close to those of the present approach as seen from Fig. 4(b).

However, the inadequacy of the 2-mode approach becomes obvious when a case of well-separated critical load is considered, e.g. column (a) (case (ii) of Table 2) with $\sigma_{c_1}/\sigma_{c_2} = 2.90$. As seen from Fig. 4(c), this theory (Ref. [9]) indicates once again serious though somewhat reduced imperfection sensitivity. This is in sharp contrast with the present theory which indicates little imperfection sensitivity and considerably higher maximum loads. Again the behavior of the column as predicted by the two theories are very different from each other. According to the 2-mode theory of Ref. [9] the column under controlled end compression attains a maximum load and goes through a well defined unloading phase. In contrast the present theory predicts a column behavior which resembles closely that of a solid Euler column with deflections increasing at an enormous rate with respect to the load carried which approaches an asymptotic value. This behavior which is observed in this study for all columns with $\sigma_{c_1}/\sigma_{c_2}$ in the vicinity of 1.5 and above, is similar to that predicted by Koiter for Tvergaard panel[5].

Influence of $\sigma_{c_1}/\sigma_{c_2}$

The column section (b) differs from section (a) in only one respect, i.e. the thickness of the web of the latter is twice that of the former. As a result a huge difference occurs

Table 3. Comparison of the performance of I-section columns having sections (a)
and (b) (Table 2)

Imperfection		Case (i)†		Case (ii)†	
ξ_1‡	$\bar{\xi}_2$	Section (a)‡ σ_u/σ_{c_2}	Section (b)‡ σ_u/σ_{c_2}	Section (a) σ_u/σ_{c_2}	Section (b) σ_u/σ_{c_2}
0.1	0.05	0.840	0.930	1.655	1.757
0.5	0.05	0.755	0.854	1.639	1.727
1.0	0.05	0.692	0.798	1.618	1.697
0.1	0.20	0.741	0.868	1.649	1.749
0.5	0.20	0.686	0.808	1.633	1.722
1.0	0.20	0.650	0.760	1.612	1.692

† Case (i): $\sigma_{c_1}/\sigma_{c_2} \simeq 1.06$, Case (ii): $\sigma_{c_1}/\sigma_{c_2} \simeq 2.90$; for both the sections.
‡ Section (a): $\sigma_{c_3}/\sigma_{c_2} = 1.21$, Section (b): $\sigma_{c_3}/\sigma_{c_2} = 2.80$.

between the values of $\sigma_{c_3}/\sigma_{c_2}$ of the two sections, these being 1.21 and 2.81 respectively for sections (a) and (b). The influence of this parameter can be seen in the values of σ_u/σ_{c_2} as obtained for the two columns for given values of $\sigma_{c_1}/\sigma_{c_2}$. These results are given in Table 3 for various levels of initial imperfections. Note that overall imperfections are given as fractions of $l/1000$. The values of σ_u/σ_{c_2} for column (b) are consistently higher than those of column (a). The vicinity of the two local critical stresses is thus seen to be an aggravating factor in the interaction.
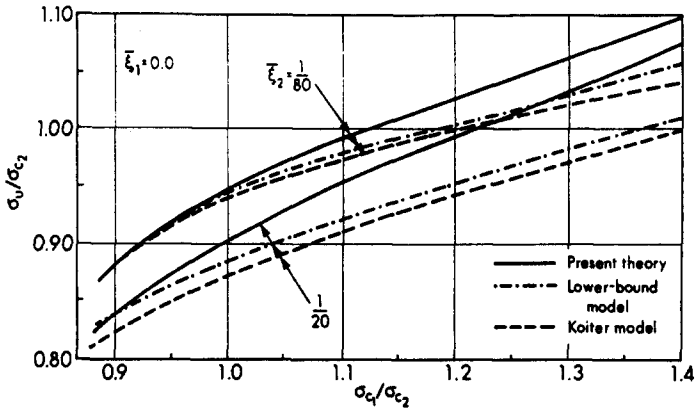
Square box column

Figures 2(c) and (d) show the primary and the secondary local modes of a box column. The ratio of the maximum load to the primary local critical load (σ_u/σ_{c_2}) is plotted against $\sigma_{c_1}/\sigma_{c_2}$ in Figs. 5(a) and (b). Figure 5(a) illustrates the effect of local imperfections only and Fig. 5(b) illustrates the effect of overall imperfections for a fixed value of local imperfection, viz. $\bar{\xi}_2 = 1/40$. Note that the overall imperfection amplitudes are now specified as percentages of the radius of gyration, r, viz. 2 and 8%. These results are compared with those of Koiter and van der Neut[7].

It is seen that even though there is good agreement for values of $\sigma_{c_1}/\sigma_{c_2}$ in the close proximity of 1.0 and for smaller magnitudes of imperfections, the results gradually deviate from each other giving a difference of about 15% at $\sigma_{c_1}/\sigma_{c_2} = 1.4$ for the higher overall imperfection.

One source of this divergence obviously is the "lower bound" modelling of local buckling in Koiter's approach. In order to quantify this source of discrepancy, the analysis based on the present theory was repeated using the lower bound approach to local buckling. The result is indicated in Figs. 5(a) and (b) by chain-dotted lines. The discrepancy was found to diminish with the maximum error nowhere exceeding 8% in the range considered. Further sources of discrepancy could not be identified as Koiter's approach is quite different and is based on a mechanical model to which he attributes various properties based on an asymptotic analysis. It is important to note that Koiter considers his model to be reliable only within the range of $\sigma_{c_1}/\sigma_{c_2}$ not exceeding 1.4.

Box type stiffened plate panels

The cross-section of a typical stiffened plate panel and the local modes of buckling are illustrated in Fig. 6. Table 4 gives the details of panels studied. The two panels investigated, viz. A and B, differed only in the slenderness (B/t) of the plate elements, which is 60 for panel A and 120 for panel B. The other cross-sectional dimensions, viz. D/t ($= 30$) and t_s/t are chosen to be the same; the lengths are also almost the same. Interestingly the values of $\sigma_{c_1}/\sigma_{c_2}$ also turn out to be the same. Thus the combined influences of differing values of $\sigma_{c_1}/\sigma_{c_2}$ and B/t on the panel behavior are investigated. The panel A is a case of near
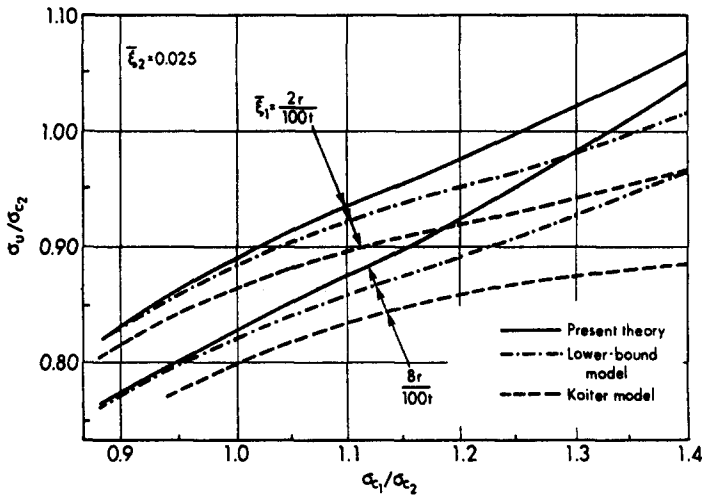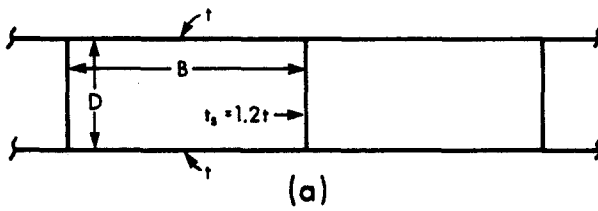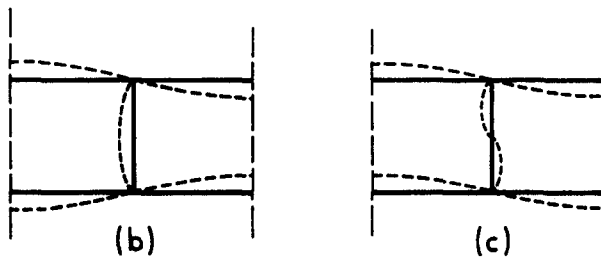
Fig. 5. The maximum load carrying capacity of square box columns vs $\sigma_{c_1}/\sigma_{c_2}$ as given by Ref. [7] and the present theory with: (a) only local imperfections; (b) combined imperfections.

Fig. 6. (a) Key dimensions of the box type panel; (b) the primary local mode; (c) the secondary local mode.

Table 4. Geometric and buckling data of box-type stiffened panels

Data	Panel A	Panel B
B/t	60	120
D/t	30	30
l/t	1200	1222
m	24	13
$\{\sigma_{c_1}/E\} \times 10^3$	1.278†	1.266†
$\sigma_{c_1}/\sigma_{c_2}$	0.997	3.71
$\sigma_{c_3}/\sigma_{c_2}$	1.13	1.13

† Obtained using a finite strip solution and includes effect of shear-lag and cross-sectional distortions

coincident buckling ($\sigma_{c_1}/\sigma_{c_2} = 1.0$) and composed of comparatively stiffer plate elements while panel B is one of well separated critical loads ($\sigma_{c_1}/\sigma_{c_2} = 3.7$), but composed of plates which are considerably more slender.

Table 5 gives the maximum loads carried by the panels for selected combinations of initial imperfections, $\bar{\zeta}_1$ and $\bar{\zeta}_2$. The maximum loads are given in dimensionless forms, viz. σ_u/E and σ_u/σ_{c_2} to facilitate comparisons of the real and relative capacities of the panels.

A study of Table 5 reveals the following features: panel A is noticeably imperfection-sensitive and panel B exhibits little imperfection-sensitivity. In contrast to panel A, panel B has considerable post-local-buckling resistance and can take loads which are more than twice the primary local critical load. In terms of actual capacity, panel A is stronger by at least 15% even in the presence of huge imperfections. But the failure is often sudden whereas ample warning in the form of huge deflections would be available before panel B collapses. But in practical metal structures collapse may take the form of extremely localized, sudden and somewhat premature plastic collapse—a factor not considered in the present paper. If imperfections are not a major consideration panel A certainly has about 30% greater capacity for about 10% more in terms of weight—a conclusion which supports "the naive optimum" approach.

CONCLUSIONS

A comprehensive analysis of interactive buckling under axial compression of thin-walled columns having doubly symmetric cross-sections has been presented. The approach duly accounts for the secondary local mode, activated by the interaction of overall mode with the primary local mode. A secondary load parameter associated with bending is introduced to ensure concentricity of axial load at the end-sections. The finite strip technique was found to greatly facilitate the accurate modelling of local buckling defor-

Table 5. Maximum loads carried by the stiffened panels

Imperfection amplitudes		Panel A		Panel B	
$\bar{\zeta}_1$*	$\bar{\zeta}_2$	$\{\sigma_u/E\} \times 10^3$	σ_u/σ_{c_2}	$\{\sigma_u/E\} \times 10^3$	σ_u/σ_{c_2}
0.1		1.158	0.903	0.771	2.258
0.5	0.01	1.073	0.837	0.755	2.211
1.0		1.010	0.788	0.737	2.158
0.1		1.037	0.809	0.769	2.252
0.5	0.10	0.990	0.772	0.753	2.205
1.0		0.957	0.746	0.735	2.152
0.1		0.982	0.766	0.765	2.240
0.5	0.20	0.955	0.745	0.750	2.196
1.0		0.933	0.727	0.732	2.143

mation. The performance of columns with typical cross-sectional configurations was examined. The predicted behavior for near-coincident buckling is similar to that obtained by the earlier asymptotic theories, but the imperfection sensitivity as given by the present theory is considerably smaller for well separated critical loads, say for values of $\sigma_{c_1}/\sigma_{c_2}$ > 1.5. In these cases the predicted behavior approaches that of a solid Euler column with a reduced buckling load.

<div align="center">REFERENCES</div>

1. A. van der Neut, The interaction of local buckling and column failure of thin-walled compression members. *Proc. XII, Int. Cong. Appl. Mech., Stanford.* Springer-Verlag, Berlin (1968).
2. J. M. T. Thompson and G. M. Lewis, On the optimum design of thin-walled compression members. *J. Mech. Phys. Solids* **20**, 101–109 (1972).
3. T. R. Graves-Smith, The ultimate strength of locally buckled columns of arbitrary length. In *Thin-Walled Steel Structures* (Edited by K. C. Rockey and H. V. Hill). Crosby and Lockwood, London (1969).
4. V. Tvergaard, Imperfection-sensitivity of wide integrally stiffened panel under compression. *Int. J. Solids Structures* **9**, 177–192 (1973).
5. W. T. Koiter and M. Pignataro, An alternative approach to the interaction between local and overall buckling in stiffened panels, IUTAM Symp., Cambridge, 1974. In *Buckling of Structures* (Edited by B. Budiansky), pp. 133–148. Springer-Verlag, Berlin (1976).
6. W. T. Koiter and M. Pignataro, A general theory for the interaction between local and overall buckling of stiffened panels. Report WTHD 83, Delft University of Technology, Holland (1976).
7. W. T. Koiter and A. van der Neut, Interaction between local and overall buckling of stiffened compression panels, Parts I, II. *Thinwalled Structures* (Edited by J. Rhodes and A. C. Walker), pp. 61–85. Granada, London (1980).
8. S. Sridharan, Doubly symmetric interactive buckling of plate structures. *Int. J. Solids Structures* **19**, 625–641 (1981).
9. S. Sridharan and R. Benito, Columns: static and dynamic interactive buckling. *J. Engng Mech. ASCE* **110**(1), 49–65 (1984).
10. B. Budiansky, Theory of buckling and post-buckling behavior of elastic structures. In *Advances in Applied Mechanics*, Vol. 14. Academic Press, New York (1974).
11. S. Sridharan, A finite strip post-local-buckling analysis of plate structures subject to nonuniform compression. *Engng Structures* **4**, 249–255 (1982).
12. S. Sridharan, A semianalytical method for the post-local-torsional-buckling analysis of prismatic plate structures. *Int. J. Num. Methods Engng* **18**, 1685–1697 (1982).
13. J. P. Benthem, The reduction in stiffness of combinations of rectangular plates in compression after exceeding the buckling load. NLL-TR S. 539 (June 1959).
14. S. Sridharan and T. R. Graves-Smith, Postbuckling analyses with finite strips. *J. Engng Mech. Div. ASCE* **107** (EM5), 869–888 (1981).

<div align="center">APPENDIX: ENERGY FUNCTIONAL</div>

Expressions of the strain fields and strain energy density for the perfect structure are given in this section in order to make explicit the underlying assumptions of the present theory. The displacement components are obtained by summing up the contributions respectively of the prebuckling state, local buckling and overall buckling. The first two taken together may be written in the form:

$$u = u_0 + \sum_{i,3} u_{ii}\xi_i^2 + u_{23}\xi_2\xi_3, \tag{ia}$$

$$v = v_0 + \sum_{i,3} v_{ii}\xi_i^2 + v_{23}\xi_2\xi_3, \tag{ib}$$

$$w = w_2\xi_2 + w_3\xi_3. \tag{ic}$$

Here, u_0 and v_0 are the prebuckling displacements, w_2 and w_3 are the normal displacements associated with the local buckling modes and the remaining terms represent the associated second order displacement fields.

Overall buckling is characterized essentially by W and U, the lateral and axial displacements of the entire cross-section. These may be written as

$$W = W_1\xi_1, \tag{id}$$

$$U = U_{11}\xi_1^2. \tag{ie}$$

The strain components of the plate middle surface take the form:

$$\varepsilon^{(m)} = \varepsilon_0^{(m)} + \sum_{i=1,2,3} \{\varepsilon_i^{(m)}\xi_i + \varepsilon_{ii}^{(m)}\xi_i^2\} + \varepsilon_{23}^{(m)}\xi_2\xi_3 \qquad (m = 1,2,3) \tag{ii}$$

with the notation $\varepsilon^{(1)} = \varepsilon_x, \varepsilon^{(2)} = \varepsilon_y$ and $\varepsilon^{(3)} = \varepsilon_{xy}$.

In the following, expressions for the various terms in (ii) are given in terms of displacements and load parameters.

Prebuckling state

$$\varepsilon_0^{(1)} = \varepsilon_{x_0} = -\lambda - Z\chi,$$

$$\varepsilon_0^{(2)} = \varepsilon_{y_0} = -\nu\varepsilon_{x_0},$$

$$\varepsilon_0^{(3)} = \varepsilon_{xy_0} = 0.$$

First order strain fields

$$\varepsilon_1^{(1)} = \varepsilon_{x_1} = -ZW_{1,xx},$$

$$\varepsilon_1^{(2)} = \varepsilon_{y_1} = -\nu\varepsilon_{x_1},$$

$$\varepsilon_1^{(3)} = 0,$$

$$\varepsilon_2^{(1)} = \varepsilon_2^{(2)} = \varepsilon_2^{(3)} = 0,$$

$$\varepsilon_3^{(1)} = \varepsilon_3^{(2)} = \varepsilon_3^{(3)} = 0.$$

Second order strain fields in individual modes

$$\varepsilon_{11}^{(1)} = \varepsilon_{x_{11}} = \left[U_{11,x} + \frac{1}{2} W_{1,x}^2 \right],$$

$$\varepsilon_{11}^{(2)} = -\nu\varepsilon_{x_{11}},$$

$$\varepsilon_{11}^{(3)} = 0,$$

$$\left. \begin{array}{l} \varepsilon_{ii}^{(1)} = \varepsilon_{x_{ii}} = u_{ii,x} + \dfrac{1}{2} w_{i,x}^2 \\[2mm] \varepsilon_{ii}^{(2)} = \varepsilon_{y_{ii}} = v_{ii,x} + \dfrac{1}{2} w_{i,y}^2 \\[2mm] \varepsilon_{ii}^{(3)} = \varepsilon_{xy_{ii}} = \dfrac{1}{2}\{u_{ii,y} + v_{ii,x} + w_{i,x}w_{i,y}\} \end{array} \right\} \quad \begin{array}{l} i = 2,3 \\[4mm] \text{(no sum on } i\text{).} \end{array}$$

Mixed second order strain fields

$$\varepsilon_{12}^{(1)} = \varepsilon_{x_{12}} \simeq 0,$$

$$\varepsilon_{13}^{(1)} = \varepsilon_{x_{13}} \simeq 0,$$

$$\varepsilon_{12}^{(2)} = \varepsilon_{13}^{(2)} = \varepsilon_{12}^{(3)} = \varepsilon_{13}^{(3)} = 0,$$

$$\varepsilon_{23}^{(1)} = \varepsilon_{x_{23}} = u_{23,x} + w_{2,x}w_{3,x},$$

$$\varepsilon_{23}^{(2)} = \varepsilon_{y_{23}} = v_{23,y} + w_{2,y}w_{3,y},$$

$$\varepsilon_{23}^{(3)} = \varepsilon_{xy_{23}} = \frac{1}{2}\{u_{23,y} + v_{23,x} + w_{2,x}w_{3,y} + w_{2,y}w_{3,x}\}.$$

Expressions for the strain energy density

The total strain energy is the sum of the bending energy and energy of inplane deformation.
Bending energy of local modes:

$$\Pi_1 = \sum_{i=2,3} D\{w_{i,xx}^2 + w_{i,yy}^2 + 2\nu w_{i,xx}w_{i,yy} + 2(1-\nu)w_{i,xy}^2\}. \tag{iii}$$

Strain energy of inplane deformation (including bending energy of the overall mode):

$$\Pi_2 = \frac{Et}{2(1-\nu^2)}\{\varepsilon_x^2 + \varepsilon_y^2 + 2\nu\varepsilon_x\varepsilon_y + 2(1-\nu)\varepsilon_{xy}^2\}. \tag{iv}$$

Thus $\Pi = \Pi_1 + \Pi_2$.

For the structure with imperfections in the modes of buckling, ξ_i^2 is replaced by $\xi_i^2 + 2\xi_i\bar{\xi}_i$ and $\xi_2\xi_3$ by $\xi_2\xi_3 + \xi_2\bar{\xi}_3 + \xi_3\bar{\xi}_2$ in eqn (ii).